

## Some results of gradient electromagnetic sounding in Doldrums Mid-Atlantic Ridge fracture

V.S. Shneyer, I.L. Trofimov, Yu.M. Abramov, M.S. Zhdanov, V.A. Machinin  
and S.V. Shabelyansky

*Institute of Terrestrial Magnetism, Ionosphere and Radio Wave Propagation (IZMIRAN), Academy of Sciences,  
142092 Troitsk, Moscow Region, USSR*

(Received 3 July 1990; accepted for publication 10 October 1990)

### ABSTRACT

Shneyer, V.S., Trofimov, I.L., Abramov, Yu.M., Zhdanov, M.S., Machinin, V.A. and Shabelyansky, S.V., 1991. Some results of gradient electromagnetic sounding in Doldrums Mid-Atlantic Ridge fracture. *Phys. Earth. Planet. Inter.*, 66: 259–264.

The geoelectrical cross-section of the Doldrums Mid-Atlantic Ridge fracture has been investigated by means of the gradient electromagnetic sounding method.

The method of experiment at sea, observation techniques, principles of processing and interpretation of the observed data are described. As a result, the first model of the deep geoelectrical structure of the ridge zone, with a high conducting layer at a depth of 30 km, has been constructed.

### 1. Introduction

The study of the ocean floor structure, particularly in active spreading zones, is of primary importance for geodynamics and geochronology studies. In this respect, lithosphere thickness measurements, asthenosphere layer location and temperature–depth distribution are the problem areas of high interest. It is known that the lithosphere has different dates of formation on either side of the axis of transform fractures. This difference is related to the spreading speed of the Mid-Atlantic Ridge. Both lithosphere thickness studies and age determinations on transform fractures provide very important geodynamic information (Gorodnitsky, 1985). Lithosphere thickness differences are found also on both sides of Mid-Atlantic Ridge axes and have been attributed to asymmetric mantle temperature distribution (Haigh, 1974). Both lithosphere thickness and asthenosphere surface temperature may be determined by deep electromagnetic sounding (Berdichevsky and Vanyan, 1969;

Duba and Lilley, 1972), a technique that has been used successfully in litho- and asthenosphere studies in the Arctic, Pacific and Atlantic Oceans (Fonarev, 1969; Greenhouse, 1972; Trofimov et al., 1973; Trofimov, 1979; Cox 1980). There has been no electromagnetic sounding carried out previously for the Mid-Atlantic Ridge.

In November 1987, during an expedition on board the scientific research ship 'Nikolay Strakhov', deep electromagnetic soundings over the Doldrums transform fracture of the Mid-Atlantic Ridge were produced. Other geological and geophysical studies included continuous seismic profiling, multibeam echo-sounding, seismic reflection, magnetic surveying, dragging and sample analysis.

### 2. Observation techniques and equipment

Sounding measurements were based on synchronous geomagnetic field variation measure-

ments at both the sea surface and the sea bed, with further calculations of amplitude ratios, amplitude differences and phase variations between the two water levels. This technique was first introduced by Fonarev (1964), and further developed by Trofimov and Fonarev (1972), Berdichevsky et al. (1979), and by Golmshtock and Sochelnikov (1971); this technique was named 'marine gradient sounding'.

To fulfil the requirements of the method, the variations of horizontal components are to be measured as far as it is possible for them to be damped with depth, depending on the conductivity of the underlying oceanic crust and mantle. However, the accurate measurement of the sea surface geomagnetic component presents a significant technical problem. It is simpler to measure the total vector modulus  $T$  on the sea surface by means of a scalar magnetometer, which has an insignificant dependence on sensor movements. Horizontal component variations,  $\Delta H$ , are related to  $\Delta T$  and  $\Delta Z$  by the equation

$$\Delta H = (\Delta T - \Delta Z \sin I) \cos^{-1} I \quad (1)$$

where  $I$  is magnetic inclination, and  $Z$  is the vertical component.

As far as the sounding produced at latitude  $9^\circ\text{N}$ , where  $I = 18^\circ$  and  $\cos I = 0.95$  (with an error of 5%), it can be accepted that

$$\Delta H = \Delta T - \Delta Z \sin I \quad (2)$$

Ocean depth at the point of sounding was about 3000 m, while the integrated longitudinal water layer conductivity was about 12000 S. In these conditions, vertical component ( $Z$ ) variations are 'damped' almost completely at periods shorter than 24 h, and then

$$\Delta H \sim \Delta T \quad (3)$$

These variation properties for the region studied enabled us to use, at the sea surface, the scalar (proton) magnetometer.

To measure sea-bed variations the marine three-component ( $H$ ,  $D$ ,  $Z$ ) magnetometer was used. Such a combination enabled us to control the influence of the  $\Delta Z$  component, to measure field polarization, to calculate the induction vectors and measure  $H$  values at the sea bed, free from the errors of recalculation.

Thus, the  $T$  modulus variations at the sea surface were measured at 50 m depth by means of a magnetovariation module set that included a proton magnetometer, control and power blocks, and digital recorder. Measurement accuracy was about 1 nT, the time interval was 1 min, clock daily deviation was  $\pm 1$  s and operational time was 7 days.

The set at the sea bed contained a three-component flux-gate magnetometer, with blocks for compensation, control, orientation and power, and an analogous photorecorder. Variations were mea-

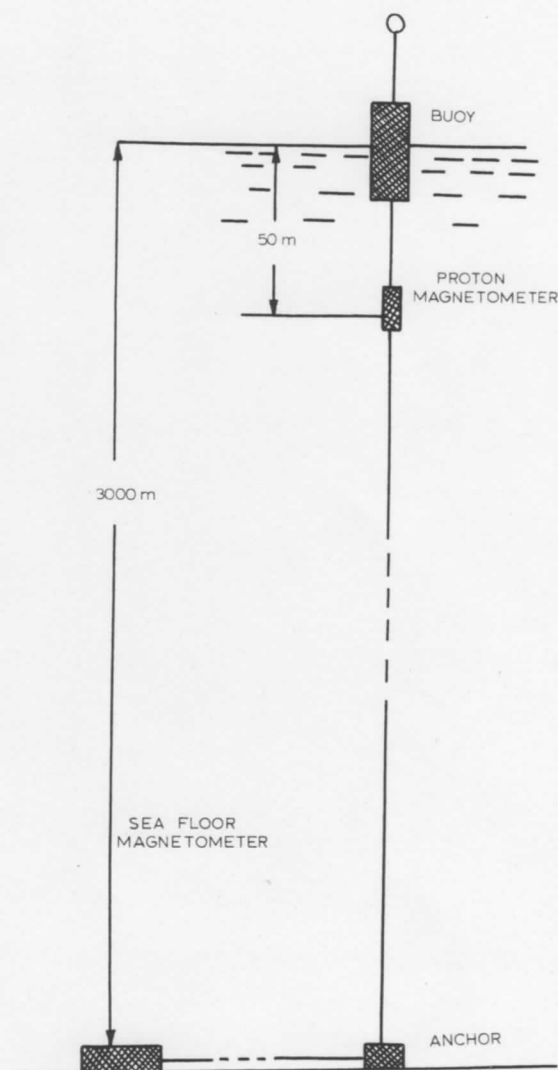


Fig. 1. Gradient sounding setting scheme.

sured up to 1 nT, with paper speed being 60 mm h<sup>-1</sup>, operational time being 10 days and clock daily deviation being  $\pm 1$  s. All the blocks of the sea-bed set were placed into one metal non-magnetic container, which in turn was placed into a light safety box.

The proton set sensor consisted of a hydrostatically discharged plastic box filled with proton-containing fluid, into which toroid inductive coil was inserted and a cable connected to an amplifier kept in a metal non-magnetic container that contained the rest of the set blocks.

A buoy with a radar reflector and flashing light was fixed at the sea surface. The buoy was connected to an anchor by means of synthetic rope with a diameter of 12 mm. The proton set was suspended from the rope and the sea-bed set was connected to the anchor by a synthetic rope 100 m long. A general view of the gradient buoy station is shown in Fig. 1.

### 3. Experiment

On 20 November 1988, the gradient buoy station was fixed at 9°01'6N, 39°58'8W near the northern flank of the Doldrums fracture 50 miles from the Mid-Atlantic Ridge, in a water depth of 2923 m.

The area is characterized by a highly fractured sea floor topography. To avoid possible data distortion by false variations owing to buoy circulation in an anomalous field, the station location was selected after taking into consideration both the sea floor topography and the geomagnetic field anomaly gradient. According to the magnetic survey data obtained, the magnetic field gradient near the station did not exceed 2 nT km<sup>-1</sup>, which corresponds to the normal field gradient. Depth control was provided by echo sounding, while a satellite navigation sensing system produced the coordinate control.

On 26 November 1988 the station was taken back on board ship. During five full days, the magnetic field vector module variations at the sea surface and three-component ( $H$ ,  $D$ ,  $Z$ ) variations at the sea-bed were simultaneously registered. Analysis of the data showed that during

the first 2 days there were quiet daily variations. On the third day (23 November 1988), at about 08:00, UT there was the sudden commencement of a world-wide magnetic storm that lasted until the recording period was over. Thus, despite the short duration of the experiment a useful record was obtained, with sufficient variation for processing with regard to gradient sounding in a wide range of time spectra.

### 4. Impedance calculation technique

Determination of the sea-bed magnetotelluric impedance  $\mathcal{Z}$  was the object of the experiment. Two equations were used. The first one to show the relation between  $\mathcal{Z}$  and  $\mu$  ratio for the two  $H$  components:  $H_0$  for the sea surface and  $H_h$  for the sea-bed

$$\mu = H_0/H_h = \cosh \kappa h + \frac{\mathcal{Z}}{\mathcal{Z}_1} \sinh \kappa h \quad (4)$$

where  $h$  is water depth,  $\kappa = (-i\omega\sigma\mu_0)^{1/2}$ ,  $\mathcal{Z} = (-i\omega\mu_0)/\kappa$ ,  $\sigma$  is seawater conductivity,  $\omega$  is cyclic variation frequency,  $\mu_0$  is vacuum magnetic permeability and  $\kappa$  is the wavenumber. The second equation relates  $\mathcal{Z}$  with the difference

$$\theta = H_0 - H_h = 2 \sinh \frac{\kappa h}{2} \frac{E_{h/2}}{\mathcal{Z}_1} \quad (5)$$

where  $E_{h/2}$  is the electric field between the sensors. For ranges of sufficiently long periods,  $2 \sinh[(\kappa h/2)/\mathcal{Z}_1] \approx \sigma h = S$ , where  $S$  is the longitudinal integral electric conductivity. Then, according to calculations within the same period ranges, there is no downward variation of the seawater electric field, the error being practically negligible. That is why it could be accepted that  $E_{h/2} \approx E_h$ , where  $E_h$  is the sea-floor electrical intensity. It follows from the above that

$$\mathcal{Z} = E_h/H_h \approx \theta/S \times H_h \quad (6)$$

To determine the  $H_0$  for  $\mathcal{Z}$  calculations, eqns. (1)–(3) were used.

### 5. Data processing technique

As mentioned above the time variations registered may be divided into two sets significantly

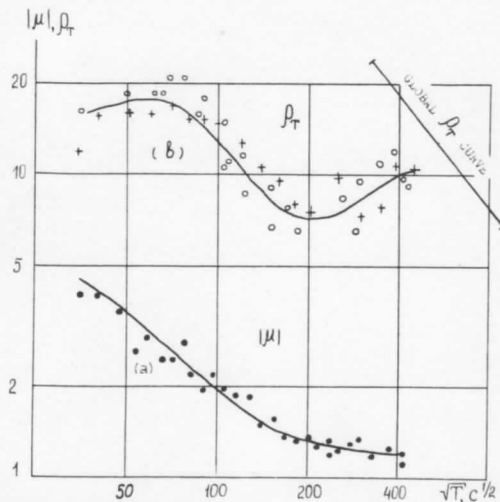


Fig. 2. Modulus of magnetic ratios (a) and apparent resistivity (b).

different in frequency spectra. The first set of 50 h duration is represented by relatively quiet solar daily variations,  $S_q$ . For this reason, the record intervals here of 24 h duration were expanded into Fourier series so that the  $S_q$  harmonics could be identified. The observed variation amplitude of  $S_q$  for horizontal components and modulus was about 200 nT. High amplitude and characteristic curve shape for  $S_q$  enabled the identification of up to the twelfth harmonics in these components. For the vertical component, only the first and second harmonics were of practical significance, with regard to eqns. (2) and (3). The second set of time variations, of 3 days duration, is represented by a

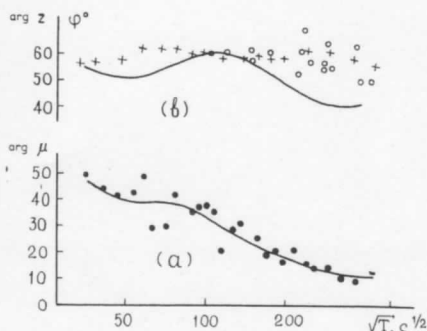


Fig. 3. Phase of magnetic ratios (a) and magnetotelluric impedance (b).

global magnetic storm with an expressed storm-time geomagnetic variation ( $D_{st}$ ) component. Storm disturbances include variations with observed periods lasting in the range of 10–15 min to several hours. Solar daily variations,  $S_D$  were also observed. This record series was harmonically expanded into a Fourier integral with further spectral harmonic identification in different components; the 'peak-to-peak' method was used. To avoid the certain errors due to the limited record length, the strongly timed spectra of the same record length were analysed. The trend was identified by the cubic polynomial calculated by the least-square procedure. The  $\theta$  value was determined by both the spectra of time series differences and the difference of the spectra. Coincident results only were processed. The values found for  $|\mu|$  and  $\arg \mu$  are shown in Figs. 2a and 3a, respectively. The apparent resistance values  $\rho_T$  and  $\arg \mathcal{Z}$ , calculated from the values found for  $\mu$  (crosses) and  $\theta$  (circles) are shown, respectively, in Figs. 2b and 3b.

## 6. Formal interpretation

For a one-dimensional horizontal-layered model of geoelectric cross-section the obtained  $\rho_T$  curve was submitted to formal interpretation. The model parameters were first roughly determined with curve extreme and asymptotic values by using proximate analytical formulae. They were further constrained by their variations, computer calculated  $\rho_T$  curve and comparison with the experimental  $\rho_T$  values. A minimum layered model was developed 'averagely' satisfying the sets of all the experimental data and corresponding to a priori information on the geoelectric cross-section. In this respect, a five-layered model turned out to be an optimum choice. Theoretical curves calculated according to this model are shown by the solid lines in the Figs. 2 and 3. This highlights the difference between theoretical curves,  $\arg \mathcal{Z}$ , and the set of experimental values. Attempts to remove this difference by sensible model complication (by increasing the number of layers) were of no use. This may be accounted for by the continuous depth-resistivity distribution, the main fea-

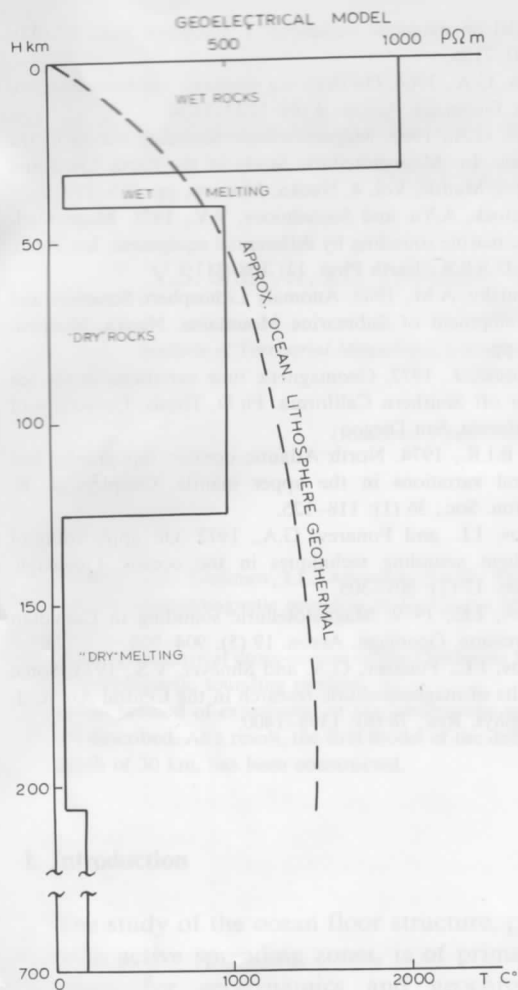


Fig. 4. Geoelectrical model.

ture of which is reflected by the horizontal-layered model.

The model is shown in Fig. 4. Its main feature is the presence of two conductive layers divided by non-conductive layers. When the model parameters were selected it was found that the shape of the  $\rho_T$  calculated curve within the total period range depends mainly on the variations of depth, thickness and resistivity values for these two layers. The acceptable deviations average 20–30%, because in this case the calculated curve will not go beyond the scattering ranges of experimental data available. The insulator resistivity values are conditional to a great extent, but they are not less than 100–200 times as much as that of the con-

ductive layers. The model parameters below the second conductive layer determined the curve behaviour for the longest periods and were selected so that the curve could coincide with that of global magnetovariation sounding.

## 7. Discussion

The first question concerns the data distortion due to the discontinuity of the geoelectric cross-section in the area of observation. Unfortunately, only single-point measurements were made. The problem thus becomes very much complicated. The only argument for small distortions may be the absence of vertical component variations for periods less than 24 to 12 h, and the presence of daily harmonics can be accounted for by the source effect. One could at least try to interpret the upper part of the model obtained.

According to geological data there is practically no sedimentary cover in the area of observations. The sea floor is highly dismembered by the set of parallel depressions, their depth being maximal along the axis of the transform fracture. The sea-floor surface is of tholeiitic and olivine lava composition.

It may be supposed that the basalt layer is substantially deep fractured and seawater saturated. This greatly reduces the rocks resistivity.

The nature of high conductivity layers occurring at depths of 30 and 125 km is of great interest. Their integral conductivities is as much as 5000 and 50000 S, respectively.

The liquid phase content is likely to be not less than 10% in order to provide a rock resistivity as much as  $2 \Omega \text{ m}^{-1}$ . This is quite probable for water solutions at temperatures of 800–900 °C and more. At depths greater than 40 km the water content may be substantially reduced with an increase of resistivity, and in conditions close to the 'dry solidus' it may go up to  $500 \Omega \text{ m}^{-1}$ .

At a 125 km depth the temperature exceeds the point of 'dry solidus' (1200 °). The melt content grows and that again reduces the resistivity down to  $2 \Omega \text{ m}^{-1}$ .

Beneath the second conductive layer the interpretation becomes problematic. If the occurrence

of the lithosphere base level is taken to be at the depth of 30 km, it could be aged (according to Gorodnitsky, 1985) as 10 millions years.

Comparison of the obtained results with similar information from the Pacific (Cox, 1980) highlights the comparatively low resistivity of the geoelectric cross-section in the Atlantic. This is undoubtedly a remarkable fact to be studied further.

In conclusion we emphasize the apparent prospects for using the described sounding technique, at least for the low-latitude regions.

### References

- Berdichevsky, M.N. and Vanyan, L.L., 1969. Prospects for deep marine sounding. *Izv. Acad. Sci., U.S.S.R., Earth Phys.*, 11: 51-56.
- Berdichevsky, M.N., Zhdanov, M.S., Trofimov, I.L. and Fonarev, G.A., 1979. *Fundamental Problems of Marine Electromagnetic Research*. Izmiran, Moscow, pp. 192-196.
- Cox, C., 1980. Electromagnetic induction in the oceans and inference on the constitutions of the Earth. *Geophys. Surv.*, 4 (1-2): 137-56.
- Duba, A. and Lilley, F.E., 1972. Effect of an ocean ridge model on magnetic variations. *J. Geophys. Res.*, 77 (35): 7100-7105.
- Fonarev, G.A., 1964. On deep sea magnetic variation distribution. *Geomagn. Aeron.*, 4 (6): 1133-1134.
- Fonarev, G.A., 1969. Magnetotelluric sounding curves in the Arctic. In: *Magnetotelluric Study of the Earth Crust and Upper Mantle*, Vol. 4. Nauka, Moscow, pp. 215-219.
- Golmshtock, A.Ya. and Sochelnicov, V.V., 1971. Magnetotelluric marine sounding by differential equipment. *Izv. Acad. Sci. U.S.S.R., Earth Phys.* 11: 108-111.
- Gorodnitsky, A.M., 1985. *Anomaly Lithosphere Structure and Development of Submarine Mountains*. Nauka, Moscow, 165 pp.
- Greenhouse, J., 1972. *Geomagnetic time variations in the sea floor off Southern California*. Ph.D. Thesis, University of California, San Diego.
- Haigh, B.I.R., 1974. North Atlantic oceanic topography and lateral variations in the upper mantle. *Geophys. J. R. Astron. Soc.*, 36 (1): 118-125.
- Trofimov, I.L. and Fonarev, G.A., 1972. On application of gradient sounding techniques in the oceans. *Geomagn. Aeron.* 12 (2): 301-305.
- Trofimov, I.L., 1979. Magnetotelluric sounding in Canadian depression. *Geomagn. Aeron.* 19 (5): 904-908.
- Trofimov, I.L., Fonarev, G.A. and Shneyer, V.S., 1973. Some results of magnetotelluric research in the Central Arctic. *J. Geophys. Res.*, 78 (8): 1398-1400.